PRAMANA
— journal of
physics

pp. 1–9

Results from STAR Experiment at RHIC

Bedangadas Mohanty (for STAR Collaboration)
Variable Energy Cylcotron Centre, 1/AF, Bidhan Nagar, Kolkata - 700064

Abstract. We present some of the important experimental results from nucleus-nucleus collision studies carried out by the STAR experiment at Relativistic Heavy Ion Collider (RHIC). The results suggests that central Au+Au collisions at RHIC has produced a dense and rapidly thermalizing matter with initial energy densities above the critical values predicted by lattice QCD for establishment of a Quark-Gluon Plasma (QGP).

Keywords. Quark-gluon plasma, Heavy-ion collisions, perturbative quantum chromodynamics

PACS Nos 25.75.Dw

1. Introduction

There has always been a considerable interest in knowing about the fate of nuclear matter when subjected to extremes of density and temperature. Particularly intriguing was the suggestion that new phases of nuclear matter could be associated with a corresponding change in the structure of the vacuum [1]. This vacuum structure is modified at high temperatures and/or densities, suggesting that quarks and gluons under such conditions would be deconfined [2]. When the energy density exceeds some typical hadronic value (> 1 GeV/fm^3), matter no longer consists of separate hadrons (protons, neutrons, etc.), but as their fundamental constituents, quarks and gluons. Because of the apparent analogy with similar phenomena in atomic physics we may call this phase of matter the QCD (or quark-gluon) plasma [3]. Lattice QCD [4] predicts a phase transformation to a quark-gluon plasma (QGP) at a temperature of approximately 175 MeV $\sim 10^{12}$ K. One of the primary goals of the relativistic heavy ion collider (RHIC) is the experimental study of the QCD phase transition by colliding heavy ions (Au+Au and Cu+Cu) at various high energies (19.6 GeV to 200 GeV).

In this manuscript we shall discuss the most recent results from one of the four experiments at RHIC [5–8], the STAR (Solednoidal Tracker At RHIC) experiment. The results are discussed in terms of the bulk properties of the hadron production (transverse momentum spectra and particle ratios), collective phenomena exhibited by the constituents of the matter and the penetrating probes in form of high transverse momentum particle production. We will also briefly discuss the recent result from the photon multiplicity detector (PMD) an Indian effort in STAR experiment at RHIC [9,10].

2. The STAR experiment

The experiments at RHIC are aimed at capturing the thousands of particles produced in nucleus-nucleus collisions whose spectra may reflect thermal, and possible chemical equilibrium of the radiating source. In order to accomplish this, STAR was designed primarily for measurements of hadron production over a large solid angle, featuring detector systems for high precision tracking, momentum analysis, and particle identification at the center of mass (c.m.) rapidity. The large acceptance of STAR makes it particularly well suited for event-by-event characterizations of heavy ion collisions and for the detection of hadron jets. The detector is operated with a uniform magnetic field of maximum value 0.5 T and consists of the following sub-detectors : Charged particle tracking close to the interaction region is accomplished by a Silicon Vertex Tracker (SVT). A large volume Time Projection Chamber (TPC) for charged particle tracking and particle identification is located at a radial distance from 50 to 200 cm from the beam axis. The TPC is 4 m long and it covers a pseudo-rapidity range $\mid \eta \mid < 1.8$ for tracking with complete azimuthal symmetry. To extend particle identification to higher momenta there is a time-of-flight (TOF) patch covering $1< \eta <0$ with $\pi/30$ in azimuth. To extend the tracking to the forward region, a radial-drift TPC (FTPC) is installed covering $2.5 < \eta < 4$, with complete azimuthal coverage and symmetry. To extend the particle identification in STAR to electromagnetic sector, there exists a full-barrel electromagnetic calorimeter (EMC) ($\mid \eta \mid < 1$) and an endcap electromagnetic calorimeter (EEMC). The photon measurements at forward rapidity ($2.3 < \eta < 3.8$) is carried out by PMD. The fast detectors that provide input to the trigger system are a central trigger barrel (CTB) at $\mid \eta \mid <1$ and zero-degree calorimeters (ZDC) located in the forward direction at $\theta <2$ mrad.

3. Bulk properties

The multiplicities, yields, momentum spectra and correlations of hadrons emerging from heavy-ion collisions, especially in the soft sector comprising particles at transverse momenta, $p_T \lesssim 1.5$ GeV/c, reflect the properties of the bulk of the matter produced in the collision. Here we only discuss about p_T spectra, particle ratios and collective flow.

The measured hadron spectra reflect the properties of the bulk of the matter at kinetic freeze-out, after elastic collisions among the hadrons have ceased. Somewhat more direct information on an earlier stage can be deduced from the integrated yields of the different hadron species, which change only via inelastic collisions. The point where these inelastic collisions cease is referred to as chemical freeze-out and usually takes place before kinetic freeze-out. The transverse momentum distributions of the different particles reflect a random and a collective component. The random component can be identified with the temperature of the system at kinetic freeze-out. The collective component which arises from the matter density gradient from the center to the boundary of the fireball created in high-energy nuclear collisions is called as collective flow. This collective flow is sensitive to the Equation of State of the expanding matter.

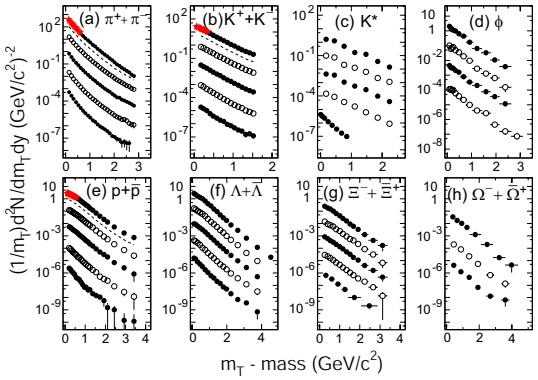

Figure 1. Mid-rapidity hadron spectra from $\sqrt{s_{NN}}$ = 200 GeV Au+Au collisions. The spectra are displayed for decreasing centrality from the top to downwards within each frame, with appropriate scaling factors applied for clarity of presentation. For K^* only, the lowest spectrum shown is for 200 GeV p+p collisions. The dashed curves in frames (a), (b) and (e) represent spectra from minimum-bias collisions. The invariant spectra are plotted as a function of $m_T - \text{mass} \equiv \sqrt{p_T^2/c^2 + \text{mass}^2} - \text{mass}$.

3.1 Transverse momentum spectra

The characteristics of the system at kinetic freeze-out can be explored by analysis of the transverse momentum distributions for various hadron species, some of which are shown in Fig. 1. In order to characterize the transverse motion, hydrodynamics-motivated fits [11] have been made to the measured spectra, permitting extraction of model parameters characterizing the random (generally interpreted as a kinetic freeze-out temperature T_{fo}) and collective (radial flow velocity $\langle\beta_T\rangle$) aspects. Results for these parameters are shown for different centrality bins and different hadron species in Fig. 2.

As the collisions become more and more central, the bulk of the system, dominated by the yields of π, K, p, appears from Fig. 2 to have lower kinetic freeze-out temperature and to develop stronger collective flow. On the other hand, even for the most central collisions, the spectra for multi-strange particles ϕ and Ω appear to reflect a higher freeze-out temperature while exhibiting considerable collectivity.

3.2 Particle ratios

Figure 3 compares STAR measurements of integrated hadron yield ratios for central Au+Au collisions to statistical model fits. In comparison to results from p+p collisions at similar energies, the relative yield of multi-strange baryons Ξ and Ω is considerably enhanced in RHIC Au+Au collisions [7]. The measured ratios are used to constrain the values of system temperature and baryon chemical potential at chemical freeze-out, under the statistical model assumption that the system is in thermal and chemical equilibrium at that stage. The excellent fit obtained to the ratios in the figure, including stable and long-lived hadrons through multi-strange baryons, is consistent with the light flavors, u, d, and s, having reached chemical equilibrium (for central and near-central collisions only)

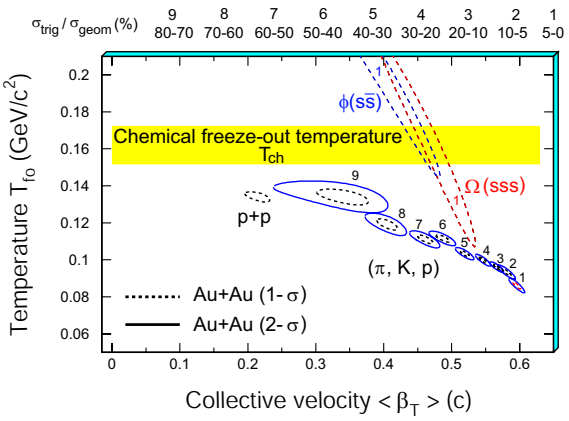

Figure 2. The χ^2 contours, extracted from thermal + radial flow fits (without allowance for resonance feed-down), for produced hadrons π, K and p and multi-strange hadrons ϕ and Ω. On the top of the plot, the numerical labels indicate the centrality selection. For π, K and p, 9 centrality bins (from top 5% to 70-80%) were used for $\sqrt{s_{NN}} = 200$ GeV Au+Au collisions. The results from p+p collisions are also shown. For ϕ and Ω, only the most central results are presented. Dashed and solid lines are the 1-σ and 2-σ contours, respectively.

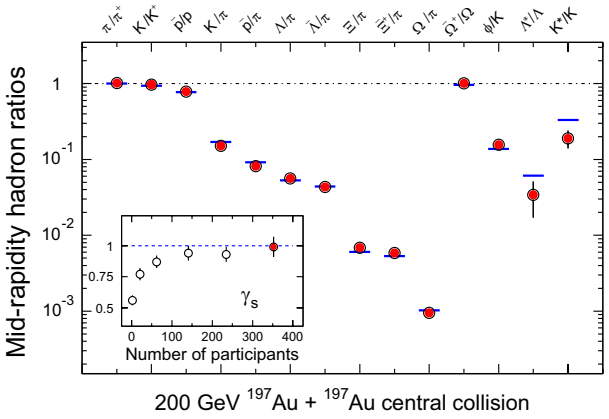

Figure 3. Ratios of p_T-integrated mid-rapidity yields for different hadron species measured in STAR for central Au+Au collisions at $\sqrt{s_{NN}}$ = 200 GeV. The horizontal bars represent statistical model fits to the measured yield ratios for stable and long-lived hadrons. The fit parameters are $T_{ch} = 163 \pm 4$ MeV, $\mu_B = 24 \pm 4$ MeV, $\gamma_s = 0.99 \pm 0.07$. The variation of γ_s with centrality is shown in the inset, including the value (leftmost point) from fits to yield ratios measured by STAR for 200 GeV p+p collisions.

at $T_{ch} = 163 \pm 5$ MeV [7]. The deviations of the short-lived resonance yields, such as those for Λ^* and K^* collected near the right side of Fig. 3, from the statistical model fits, presumably result from hadronic rescattering after the chemical freeze-out and needs to be further understood.

The saturation of the strange sector yields, attained for the first time in near-central RHIC collisions, is particularly significant. The saturation is indicated quantitatively by the value obtained for the non-equilibrium parameter γ_s for the strange sector for central collisions. The temperature deduced from the fits is essentially equal to the critical value for a QGP-to-hadron-gas transition predicted by Lattice QCD [4], but is also close to the Hagedorn limit for a hadron resonance gas, predicted without any consideration of quark and gluon degrees of freedom [12]. If thermalization is indeed achieved by the bulk matter prior to chemical freeze-out, then the deduced value of T_{ch} represents a lower limit on that thermalization temperature.

4. High p_T particle production

The most exciting results to date at RHIC are the discovery of high-p_T suppression of mesons in nucleus-nucleus collisions compared to binary collision scaled p+p collision data. This has been interpreted in terms of energy loss of quarks in a high-density medium. The other interesting aspect seen is the non-suppression of baryons or equivalently, the anomalously high p/π ratio.

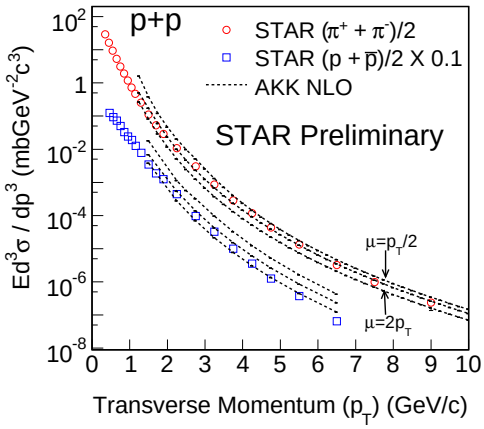

Figure 4. Midrapidity invariant yields for $(\pi^+ + \pi^-)/2$ and $(p+\bar{p})/2$ at high $p_{\rm T}$ for minimum bias p+p collisions at $\sqrt{s_{NN}} = 200$ GeV compared to results from NLO pQCD calculations using AKK (PDF: CTEQ6M) set of fragmentation functions. The calculations from AKK are for three different factorization scales: $\mu = p_{\rm T}/2$, $\mu = p_{\rm T}$, and $\mu = 2p_{\rm T}$.

The results on high-p_T suppression are usually presented in terms of the nuclear modification factor (R_{AB}), defined as:

$$R_{AB} = \frac{dN_{AB}/d\eta d^2p_T}{T_{AB} d\sigma_{NN}/d\eta d^2p_T} \quad (1)$$

where the overlap integral $T_{AB} = Nbinary/\sigma^{pp}_{inelastic}$. Where a R_{AB} value of 1 at high p_T would indicate the absence of nuclear effects, value of > 1 at high p_T would indicate effects such a transverse momentum broadening and value of < 1 at high p_T would indicate energy loss of particles passing through a dense medium. To establish the observation of $R_{AA} < 1$ at RHIC is indeed due to formation of a matter with densities well above the normal nuclear matter, it is essential to first establish the understanding of the data from p+p collision baseline, and then study the R_{AB} for d+Au collisions, various collisions centrality and particle species.

Figure 4 shows the comparison of the charged pion and proton+anti-proton spectra in p+p collisions at $\sqrt{s}$ = 200 GeV measured by STAR [13] to NLO pQCD calculations using the AKK fragmentation functions for various factorization scales. It is observed within the systematic errors in both theory and data, the results are consistent with each other.

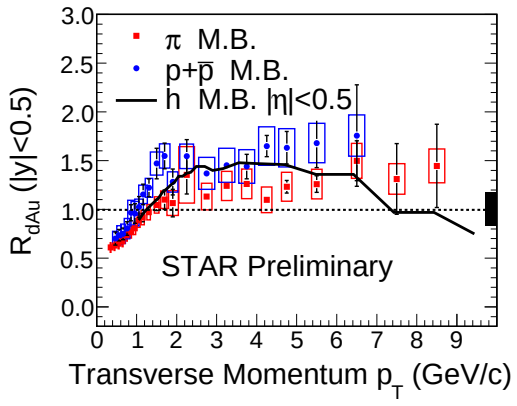

Figure 5. Nuclear modification factor $R_{\rm dAu}$ for charged pions $(\pi^+ + \pi^-)/2$ and p+$\bar{p}$ at |y| < 0.5 in minimum bias d+Au collisions at $\sqrt{s_{NN}} = 200$ GeV. For comparison results on inclusive charged hadrons (STAR). at $\mid \eta \mid < 0.5$ are shown. The shaded band is the normalization uncertainty from trigger and luminosity in p+p and d+Au collisions.

Figure 5 shows the $R_{\rm dAu}$ for charged pions ($(\pi^+$+$\pi^-)/2$) and combined proton and anti-proton (p+$\bar{p}$) in d+Au minimum-bias collisions for $\sqrt{s_{NN}}$ = 200 GeV at |y| < 0.5 [13]. The $R_{\rm dAu} > 1$ indicates a slight enhancement of high $p_{\rm T}$ charged pions yields in d+Au collisions compared to binary collision scaled charged pion yields in p+p collisions within the measured (y, $p_{\rm T}$) range. The $R_{\rm dAu}$ for $p + \bar{p}$ is again greater than unity for $p_{\rm T} > 1.0$ GeV/c and is larger than that of the charged pions.

The measurement of $\rm R_{AA}$ (0-5% Central AuAu/Scaled Minbias pp) from STAR experiment with respect to $\rm p_T$ is shown in Fig. 6. While the measurements for mesons ($\rm h^+ + h^-$, $\rm K^0_S$, ϕ) $\rm R_{AA}$ are suppressed, $\rm R_{AA}$ of strange baryons shows significant differences. Strange baryons do not show any suppression. Instead there is an enhancement and ordering with strangeness content: the higher the strangeness content, the higher the $\rm R_{AA}$ measurement in the intermediate $\rm p_T$ region. The other intersting point to note is a suppresion of more

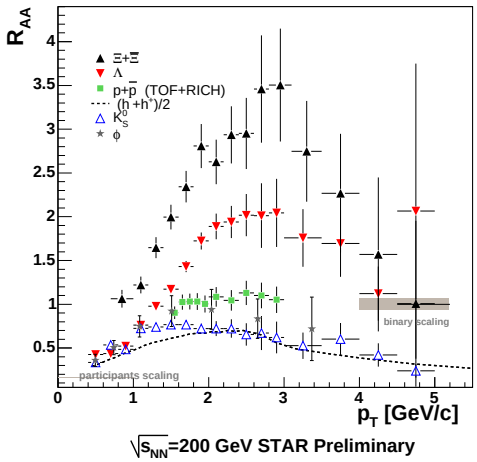

Figure 6. Nuclear modification factor, R_{AA} of $\mathrm{h}^+ + \mathrm{h}^-$, K^0_S, ϕ at $\sqrt{\mathrm{s_{NN}}} = 200$ GeV with respect to $\mathrm{p_T}$. $\mathrm{R_{AA}}$ is for 0-5% central AuAu collisions over normalized min-bias pp collisions for the given energies.

than a factor 5 when compared to results from d+Au collisions. This a is strong evidence that the suppression is not an initial state effect, but a final state effect caused by the high density medium created in the collision. Comparison to theoretical prediction [14] using the GLV parton energy loss model shows that an initial parton density $dN^g/dy = 1100$ is needed to explain the data, which corresponds to an energy density of approximately 15 GeV/fm^3. Thereby providing so far the best evidence of a dense partonic matter formed at the initial stages of nucleus-nucleus collisions at RHIC.

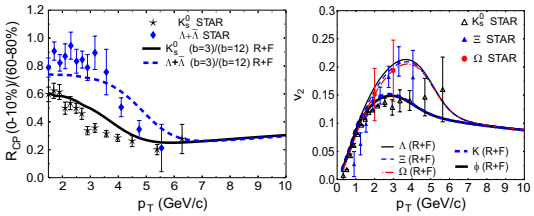

Figure 7. Comparisons of calculations in the Duke quark recombination model with STAR measurements of (a) R_{CP} and (b) v_2 for strange mesons and baryons. "R+F" denotes the sum of recombination and fragmentation contributions. Comparison of the solid and broken curves in (b) reveals a weak mass-dependence in the calculations, superimposed on the predominant meson-baryon differences.

The baryon and meson differences observed at intermediate p_T region is explained reasonably well (at least the trends) by assuming that hadron formation at moderate p_T proceeds via two competing mechanisms: the coalescence of n_q constituent quarks at transverse momenta $\sim p_T/n_q$, drawn from a thermal (exponential) spectrum, plus more traditional fragmentation of hard-scattered partons giving rise to a power-law component of the spectrum. This comparison to STAR data is shown in the Fig. 7. This can be viewed as

another evidence of a matter formed at RHIC which is partonic with collectivity exhibited at partonic level.

5. Indian contribution in STAR experiment at RHIC

The main Indian group contribution to RHIC is in the form of a photon multiplicity detector (PMD). First results on photon distribution in the forward region at 62.4 GeV energy recently became available from the PMD in the STAR experiment [10]. In Fig. 8 we have plotted the photon pseudorapidity distribution per participant nucleon in Au+Au collisions at 62.4A GeV as a function of η-y$_{beam}$ for central collisions. Also superposed are the data from the WA98 experiment for the Pb+Pb collisions at 17.A GeV c.m. energy, from the WA93 experiment for S+Au collisions at 20.A GeV c.m. energy and from the UA5 experiment for $p + p$ collisions at 546 GeV. The data at SPS and at RHIC are found to be consistent with each other, suggesting that photon production follows the limiting fragmentation hypothesis. It is further found that the data are consistent with impact parameter and energy independent behavior of longitudinal scaling.

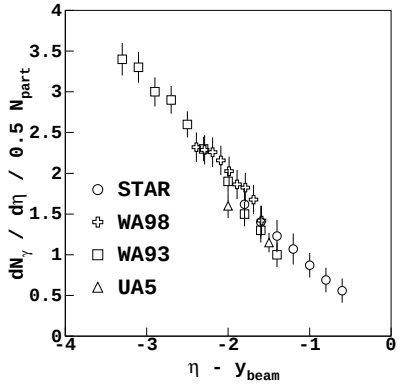

Figure 8. Limiting fragmentation in the photon production.

6. Summary

In summary, there is compelling experimental evidence (some more experimental evidence can be found in Refs. [5–8]) that heavy-ion collisions at RHIC produce a state of matter characterized by very high energy densities, density of unscreened color charges ten times that of a nucleon, large cross sections for the interaction between strongly interacting particles, strong collective flow, and early thermalization. Measurements indicate that this matter modifies jet fragmentation and has opacity that is too large to be explained by any known hadronic processes. This state of matter is not describable in terms of ordinary

color-neutral hadrons, because there is no known self-consistent theory of matter composed of ordinary hadrons at the measured densities. The most economical description is in terms of the underlying quark and gluon degrees of freedom. Models taking this approach have scored impressive successes in explaining many, but not all, of the striking features measured to date. Determining whether the quarks and gluons in this matter reach thermal equilibrium with one another before they become confined within hadrons, and eventually whether chiral symmetry is restored, are two among many profound questions one may ask as we move from the initial discovery phase of dense partonic matter to the next phase of probing the properties of the matter created at RHIC. Indian photon multiplicity detector at RHIC has successfully taken data. The first results from this detector has contributed to significant understanding of the particle production mechanism at RHIC [10].

References

[1] T. D. Lee, *Trans. N. Y. Acad. Sci. Ser.2* **v.40** (1980) 0111.
[2] J. C. Collins, M. J. Perry, *Phys. Rev. Lett.* **34** (1975) 1353.
[3] E. V. Shuryak, Phys. Rept. 61 (1980) 71.
[4] F. Karsch, Lecture Notes in *Physics* **583** (2002) 209.
[5] BRAHMS Collaboration, I. Arsene et al., *Nucl. Phys. A* **757** (2005) 1.
[6] PHOBOS Collaboration, B.B. Back et al., *Nucl. Phys. A* **757** (2005) 28.
[7] STAR Collaboration, J. Adams et al., *Nucl. Phys. A* **757** (2005) 102.
[8] PHENIX Collaboration, K. Adcox et al., *Nucl. Phys. A* **757** (2005) 184.
[9] Aggarwal M.M. et al.,*Nucl. Instr. Meth.* **A499** (2003) 751.
[10] Adams J. *et al.*, STAR Collaboration, *Phys. Rev. Lett.* **95** (2005) 062301.
[11] E. Schnedermann, J. Sollfrank, and U. Heinz, *Phys. Rev. C* **48** (1993) 2462.
[12] R. Hagedorn, *Nuovo Cim. Suppl.* **3** (1965) 147.
[13] STAR Collaboration, J. Adams et al., nucl-ex/0601033 (Physics Letters in press).
[14] I. Vitev and M. Gyulassy, *Phys. Rev. Lett.* **89** (2002) 252301.
[15] B. Müller, *nucl-th/0404015*; R.J. Fries, B. Muller, C. Nonaka, and S.A. Bass, *Phys. Rev. Lett.* **90** (2003) 202303.